EasyChair Preprint

№ 13970

A Hybrid Approach for Maximum Power Point Tracker on PV Systems.

Ely Ondo Ekogha and Pius Adewale Owolawi

July 15, 2024

A Hybrid Approach for Maximum Power Point Tracker on PV Systems.

Ely Ondo Ekogha†
Computer system engineering
Tshwane University of Technology
Pretoria, Gauteng, South Africa
OndoEkoghaE@tut.ac.za

Pius Owolawi
Computer system engineering
Tshwane University of Technology
Pretoria, Gauteng, South Africa
OwolawiPA@tut.ac.za

Abstract—As the usage of photovoltaic is emerging to palliate the degradation of the atmosphere and the natural environment. Photovoltaic (PV) systems appear to be the key for green energy production for households and industrial sectors. However, due to the dynamic change of load for a PV system or the variations of weather conditions, most PV systems are equipped with a maximum power point tracker (MPPT) to operate at their optimum capabilities. However, the efficiency of the MPPT controller varies from the techniques and algorithms used thus affecting the operations of the PV system. This paper proposes a hybrid technique based on Artificial neural network (ANN) combines with perturbation and observation (P&O) or incremental conductance (IC) algorithms using MATLAB Simulink for tracking the ideal maximum power point under uniform and sudden change of weather conditions. A comparison is depicted with conventional techniques, the findings suggest that the hybrid ANN-IC technique has an improved accuracy of 98% and response time 0,154 seconds to MPP under uniform weather. The model presents a fast-tracking response under rapidly changing conditions for a convergence time of $\mathbf{1.013}\ \boldsymbol{\mu s}$.

Keywords—Maximum power point (MPP) tracker, artificial neural network (ANN), perturbation and observation (P&O), incremental conductance (IC).

I. INTRODUCTION

Moving toward renewable energy sources has quickened, because of increased awareness of issues such as global warming which affect our environment such as air pollution, nature degradation, and greenhouse gases on the atmosphere. When compared to other clean energy sources, solar photovoltaic (PV) energy has stood out as being particularly accessible [1]. A survey on solar energy technology adoption and diffusion was conducted by authors [2] on micro-, small, medium enterprises where important criteria were deducted such as the enterprise size, the ease of use as well as the reliability of the system in contrast with the cost of production. It was demonstrated in [3], that the trends towards rooftop solar PV installation is galvanized by local governments for environment preservation, education and household's perception. In fact, authors in [4], describe that energy harvest from PV systems has become more common as a result of lower PV module prices, intentional government provisions, and innovative business models in homes, businesses, and grid power systems. However, PV system's efficiency mainly depends on several factors including the system configuration, the shading patterns, the irradiation and temperature as well as the aging effect [5]. Authors in [6], describe that PV system's performance is strongly dependent on ambient temperature and the solar radiation which are unevenly dispatched over the panel module causing multiples local maximum power points. Also, if a solar panel is directly coupled to a load, its operational point is the intersection of the PV module's I-V curve and the load curve. However, this operating point may not always correspond to the PV module's maximum power point (MPP). [7].

Therefore, to get the most power out of the PV system, an MPP tracking algorithm that seeks to find the general peak point under all conditions and fine tune the array's voltage or current to this point is necessary. In addition, to control the voltage or current of the array, a DC-to-DC converter connects the PV array to the load [1, 8, 9]. The maximum output power is obtained by controlling the duty cycle from the converter injected in the PV panel to meet the highest point of the P-V curve characteristics [10]. Some guidelines are provided by authors in [10, 11], for a proper MPPT system including several points such as:

- The MPPT system should be simple and must be easily adapted to different types of PV systems.
- The MPPT system must have the best possible accuracy for the true global MPP and tracking efficiency in various weather conditions.
- A rapid response in sudden change of weather conditions when tracking the MPP is important.
- A minimum or no oscillations around the MPP is also mandatory.

The MPPT management technique is a difficult subject of study because hardly any methods could be acknowledged as the best. For starters, most techniques have not been tested and confirmed in real-time. Second, all operating limitations are not taken into account, and results are supplied with only

a few or none at all. Third, when comparing the cost of power produced by a PV array to alternative options, the MPPT approach must be designed with cost-effectiveness in mind [11]. Therefore, this paper will outline the different techniques and findings for MPPT system from various authors in section 2, then our model and considerations will be presented in section 3. In section 4 we will discuss the findings and interpretation of our system and the paper will be concluded in section 5.

II. LITERATURE REVIEW

Several techniques and algorithms have been used by various authors to fulfil the characteristics of the maximum power point tracker system, each carries its advantages and drawbacks. Researchers in [12], classifies MPP algorithms based on measurements, calculations, intelligence scheme and hybrid scheme. Measurement algorithms work by performing computation of the PV's voltage or current and comparing the outcomes to previous calculations or a predefined MPP parameter. Calculation algorithms depend solely on a predefined formula of the MPP, the intelligent scheme refers to advanced computations that can predict the MPP and the hybrid scheme refers to the mixture of conventional methods and advanced intelligent algorithms. Authors in [10], have categorized techniques for MPP as conventional and modern techniques. Conventional techniques include perturbation and observations (P&O), incremental conductance (IC), fractional open circuit voltage/short circuit current (FOVC) and hill climbing (HC). Meanwhile modern techniques include artificial neural, network (ANN) techniques, fuzzy logic (FL), and metaheuristic-based techniques.

Research for an improved maximum power point tracking controller for PV systems using artificial neural network was conducted in [13],the authors present a model based on ANN with feedback propagation for a faster response time for MPP tracking to respond to environmental changes. The model uses solar radiation and temperature data as well as temperature coefficients of short current (I_{SC}) and open voltage (V_{OC}) to find the optimum output power. The model's results are compared to simplified method of perturbation & observation (P&O) to show its superior tracking efficiency of 95.51% for ANN against 85.99% for P&O. Fuzzy logic and adaptive neuro fuzzy logic interference system (ANFIS) algorithms were used in papers [14, 15] for MPP tracking and control. The simulations were compared to conventional methods for MPP such as incremental conductance and P&O on criteria such as speed, efficiency, stability, and precision with an overall superiority of the models proposed. Similarly, investigation in paper [16] were made to determine the MPP under partial shaded conditions using a hybrid constant-voltage and fuzzy logic methods which consist of observational tracking of MPP using fuzzy logic under constant irradiance while under partial shaded the MPP is determined using constant voltage method. The results claim an improvement of output power of 10% compared to the conventional P&O method. However, approaches based on fuzzy logic algorithm have challenges in both design and hardware implementation; precision is low under low irradiance conditions; periodic tuning is necessary; and excellent system understanding is required for building membership functions. These complexities make the methods system-dependent [11]. An MPP controller algorithm using neural network was investigated in paper [17], whereby the authors used the variations of power and voltage given by P&O algorithms to feed the neural network in order to determine the duty cycle required for the system. The paper claims to have a better response time to the variation of irradiance of 0,035 seconds and good tracking efficiency. A gene expression programming based MPPT technique is developed for micro inverter application in paper [18], the authors claim that the genetic algorithm based MPPT system is less complex since it is derived from an equation. The obtained results claim that the suggested MPPT technique shows promising improvements in the overall system's efficiency, overshoot rate, convergence speed, tracking accuracy, and dynamic response. The system's efficiency shows an increase of 4% on average for the total system. Overshoot is decreased by at least 0.6 A, while convergence speed is raised by 1.4 seconds. A comparative study between P&O and incremental conductance algorithms for MPP was performed in research [19], the authors compared both techniques over efficiency, voltage, current and output power using three types of DC-DC converter under various irradiances. The result demonstrates a net superiority of the incremental conductance methods. An improved particle swarm optimization (PSO) method for MPPT under partial shading or failure conditions was developed in [20], the model was constructed for tracking speed and accuracy using a PIC18F8720 and PSO exponential form parameter control to reduce iteration numbers and improve tracking effectiveness. This strategy used exponential increases or decreases in the cognition-only learning factor, the social-only learning factor, and the inertia weight. The proposed method claims to reduce the number of iterations to 21,1 while a traditional PSO stands at 38,3. Another technique using a tracking electronic device was developed in paper [21] for obtaining the maximum power of a PV system. The system includes two stepper motors controlling two PV panels via an AT Mega IC which tracks the sun from 9 AM to 4PM. The results display an improved augmentation of output voltage from tracking compared to no tracking device. An economic and technical classification of MPPT methods was investigated in paper [22]. The authors claimed that methods such as curve fitting, look up table, fractional shot circuit current (FSCC), fractional open circuit voltage (FOCV), constant voltage (CV), and load base method are suitable for small-scale applications, where cost trumps efficiency and precision, such as household solar chargers. Meanwhile, methods involving perturbation, differential, numerical and conductance are all appropriate for commercial and everyday applications. State space and intelligent approaches are used in high-sensitivity situations where efficiency, accuracy, and speed are critical, such as in space

applications. Another economical study for MPPT techniques on wind and solar systems was developed in [23], the chosen criteria were the capacity of utilization, the system cost, the energy generated, the energy produced revenue, the payback time period, and the stability of the method. The analysis was made on methods including P&O, IC, HC, FL, ANN and PSO. The result claimed that particle swarm method is the best overall from the chosen criteria.

Different methods were elaborated for tracking the MPP on PV systems, each with their own perspectives and analysis reports. The following section will discuss the implementation and analysis of the proposed methodology.

III. Model Presentation

A. *System architecture*

*1) Partial shading conditions (PSC):*To maximize PV system energy generated, PV panels are arranged in parallel to increase the output current or they can be connected in series to maximize the output voltage of the system [24]. However, in industrial PV systems some PV panels might not receive the same amount of radiations as other in the system due to clouds, trees around some panels, or other environmental factors thus creating hotspots or resistances where energy dissipation occurs, this phenomenon is called partial shading [25]. If PSC happens on the series-connected PV strings, the cell with the lower irradiance value will operate as a load and waste some power, causing the cell temperature to rise. As a result, the cell will be destroyed. To remedy this issue, bypass diodes are linked across the PV modules, bypassing the less shaded modules during the PSC. In addition, a blocking diode is connected at the output of the combined panels to prevent current reversal [23, 26]. The following figures depict the PV system configuration under PSC and the output effect on the I-V/P-V curve characteristics. The PV system uses Kyocera solar KC200GT for four different radiations (1000 W/m^2, 750 W/m^2, 500 W/m^2, 250 W/m^2).

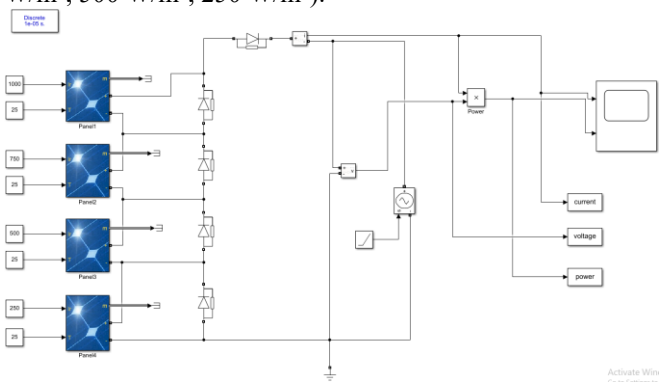

Figure 1: PSC Simulink diagram under various irradiations (1000 W/m^2, 750W/m^2, 500 W/m^2 and 250 W/m^2).

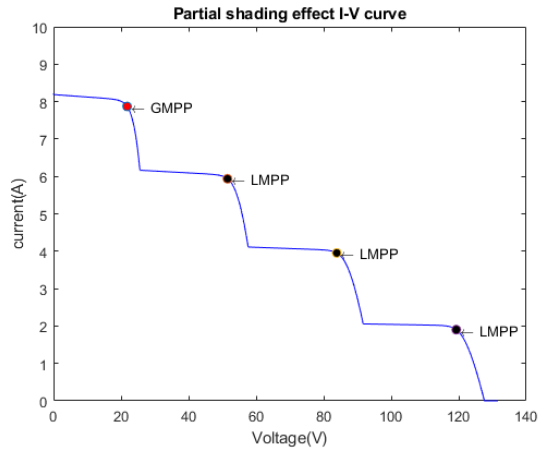

Figure 2: Effect of PSC on I-V characteristics.

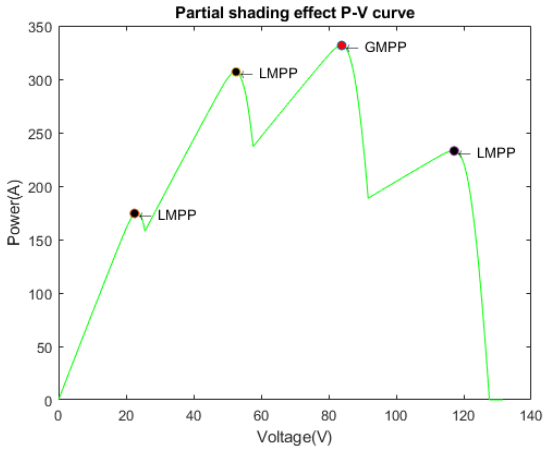

Figure 3: Effect of PSC on P-V characteristics.

The MPPT controller should be able to converge rapidly to the global MPP (GMPP) with maximum efficiency.

2) PV cell model. The solar cell is the basic unit of a photovoltaic module, and it is responsible for directly converting the sun's rays or photons into electric power [27]. The solar cell is defined as a p-n junction with nonlinear properties, whereby a current source is connected in parallel with a diode D and a resistance R_{SH}, in addition, a resistance R_S equivalents to the series connected cell is added to complete the circuit of a solar cell as depicted in the figure 3 [24].

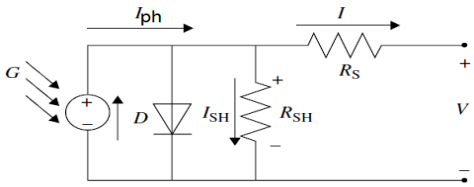

Figure 4: Equivalent circuit of a solar cell.

The output current is defined by the following equations[24].

$$I = I_{ph} - I_o\left(\exp\left(\frac{V+IR_S}{a*V_t}\right) - 1\right) - \frac{V+IR_S}{R_{SH}} \quad (1)$$

$$I_{ph} = I_{sc\_STC} + K_i(T - T_{STC})\frac{G}{G_{STC}} \quad (2)$$

$$V_t = \frac{k*T}{q} \quad (3)$$

$$V_{t1} = \frac{k*T_{STC}}{q} \quad (4)$$

$$I_o = I_{o\_STC}\left(\frac{T}{T_{STC}}\right)^{\frac{3}{a}}\left[\exp\left(\frac{-q*Vg}{a*k} * \left(\frac{1}{T} - \frac{1}{T_{STC}}\right)\right)\right] \quad (5)$$

$$I_{o\_STC} = \frac{I_{sc\_STC}}{\exp\left(\frac{V_{oc}}{a*V_{t1}}\right)-1} \quad (6)$$

$$X_V = \frac{I_{o\_STC}}{a*V_{t1}} * \exp\left(\frac{V_{oc}}{a*V_{t1}}\right) \quad (7)$$

$$dV/dI_{Voc} = -\frac{Vg}{2*N_s} \quad (8)$$

$$R_s = -dV/dI_{Voc} - \frac{1}{X_V} \quad (9)$$

Where I, I_{ph} and I_o are respectively the output current from the panel, the photo-current generated from the cell p-n junction and the reverse current from the diode. V, Vt and Vg are the PV cell voltage, thermal voltage and the band gape voltage, I_{SC_STC}, V_{OC_STC}, T_{STC}, and G_{STC} are the short current, open circuit voltage, temperature and irradiance under standard test conditions (STC) defined by a temperature of 25°C, irradiance of 1000 W/m^2 and wind speed of 1 m/s. Ki is coefficients for short current, while a is a constants for ideality factor(1,2 for monocrystalline, 2 for polycrystalline), q is a constant for electric charge ($1{,}6 * 10^{-19}C$) and k is the Boltzmann constant ($1{,}38 * 10^{-23}J/K$).

Programmatically on MATLAB, the solution for calculating the output current given that the parallel resistance is extremely high is defined as:

$$I = I + \frac{I_{ph} - I - I_o\left(\exp\left(\frac{V_C+IR_S}{V_t}\right)-1\right)}{\frac{I_oR_S\left(\exp\left(\frac{V_C+IR_S}{V_t}\right)-1\right)}{V_t}+1} \quad (1)$$

The following figure describes the curves for I-V and P-V:

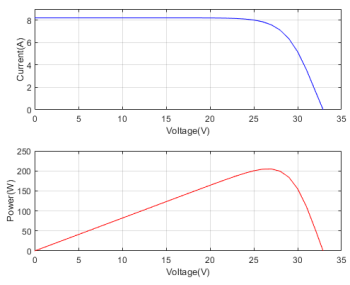

Figure 5: I-V and P-V characteristics.

3) Boost converter application. To transfer PV power effectively from the panels to the load at optimum operating conditions, MPPT controllers are built-in with a DC-to-DC converter [28]. These converters are generally designed as a buck converter to step down the input voltage, a boost converter to step up the input voltage or a cuck converter to inverse the polarity of the input signal [19]. For the purposes of this paper, our simulations will be based on a DC-to-DC boost converter to maintain the optimum operating power levelled at the input and output. Boost converters are known for their stabilities and efficiency because their can easily regulate the load impedance effect from the input voltage of the PV system [29].

A design for a boost converter is given in figure 6.

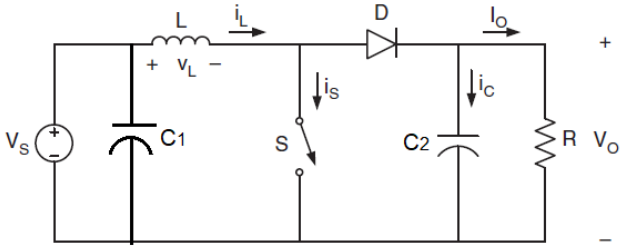

Figure 6: Boost converter diagram.

A booster converter is generally composed of a voltage source V_S which will be replaced by our PV generated power, an input capacitor C_1, a boost inductance L, a diode D, a switch S, an output capacitor C_2 and an output resistance R. When switch S is turned on, the current in the boost inductor grows linearly. Meanwhile, diode D is turned off. When switch S is turned off, the energy stored in the inductor is released to the input RC circuit via the diode. The Faraday's law equation is therefore given for the boost inductor [30]:

$$V_S * d * t = (V_O - V_S)(1 - d) * t \quad (11)$$

$$\frac{V_S}{V_O} = \frac{1}{1-d} \quad (12)$$

Where Vo is the output voltage, t is the period given by the switching *on-off* frequency of switch S and d is the duty cycle. The boost inductance L is defined by $L > L_b$:

$$L_b = \frac{d*R(1-d)^2}{2f} \quad (13)$$

Author [31], define the boost inductance formula as:

$$L = \frac{V_S(V_O - V_S)}{f*V_O*\Delta I_L} \quad (14)$$

$$\Delta I_L = \frac{V_O}{V_S} * I_{out\_max} * (0.2\ to\ 0.4) \quad (15)$$

Where ΔI_L is the inductor ripple current which is estimated between 20% to 40% of the output current I_{out_max}.

The minimum value for the output capacitor C_2 is given by [30]:

$$C_{min} = \frac{d*V_o}{V_r R f} \quad (16)$$

Where f is the switching frequency, Vr is allowable ripple voltage given by:

$$V_r = V_o * p \quad (17)$$

Where p is the ripple percentage of the output voltage Vo. The input capacitor C1 is chosen to be two times greater than the output capacitor for proper operation.

$$C_1 \approx C_2 * 2 \quad (18)$$

To manage the switch state when utilizing a DC-DC converter for tracking the maximum power on buck, or boost type, a proper control signal is necessary. The inclusion of a control circuit to the converter and the use of pulse width modulation (PWM) techniques are standard methods for producing the switch control signal. [28].

B. *Perturbation & observation and incremental conductance models*

1) Perturbation & observation (P&O) algorithm:. Among the conventional methods for MPPT controller, P&O method has been the most used on PV systems because of its simplicity, low cost and easy implementation, in addition this method does not require a deep knowledge of the PV system's parameters [14, 24]. The principle of the algorithm is to alter the voltage or current of the PV module in fractional steps and observe the effect on the produced power. The power of the previous step is then compared to the power of the following step to determine whether to increase or decrease the voltage or current [32]. If the variation of power ΔP_{pv} is positive, the fractional perturbation should be maintained in the same direction, whereas if ΔP_{pv} is negative the perturbation should be done in the opposite direction [24], a constant C of $0{,}1V$ for the perturbation is usually recommended. The following figure represents the flow chart of the algorithm.

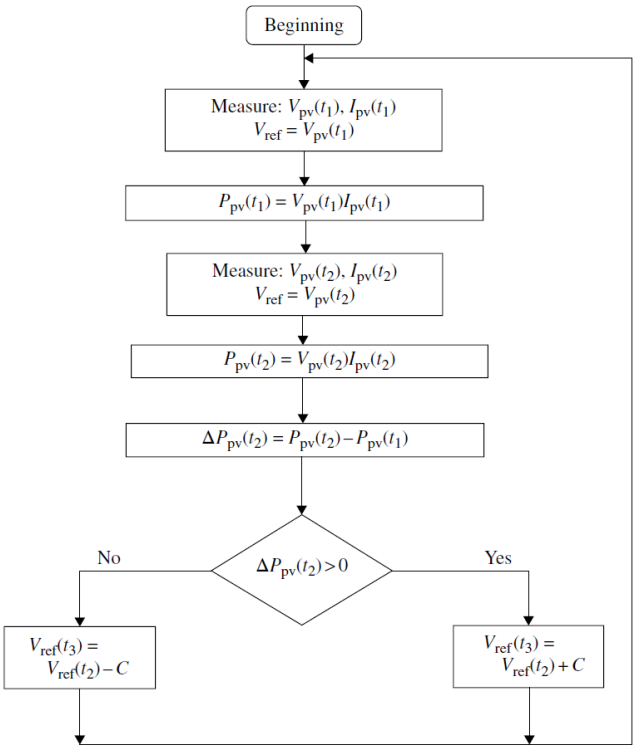

Figure 7: P&O algorithm for MPPT.

The drawback using this method is the ongoing oscillation around the MPP which increases dissipation.

2) Incremental conductance (IC) algorithm. This method has advantage to track the MPP under fast changing of irradiances and does not oscillate around the MPP although it also uses a constant for PV power iteration [19]. IC relies on the differentiation of power with respect to voltage in the following equations:

$$\frac{dP_{pv}}{dV_{pv}} = I_{pv}\frac{dV_{pv}}{dV_{PV}} + V_{pv}\frac{dI_{pv}}{dV_{PV}} = I_{pv} + V_{pv}\frac{dI_{pv}}{dV_{PV}} = 0 \quad (19)$$

$$\frac{dI_{pv}}{dV_{PV}} = -\frac{I_{pv}}{V_{pv}} \quad (20)$$

From the equation above:

- If $\frac{dP_{pv}}{dV_{pv}} > 0 \rightarrow \frac{dI_{pv}}{dV_{PV}} > -\frac{I_{pv}}{V_{pv}}$, then the system is operating on the left side of the MPP.
- If $\frac{dP_{pv}}{dV_{pv}} < 0 \rightarrow \frac{dI_{pv}}{dV_{PV}} < -\frac{I_{pv}}{V_{pv}}$, then the system is operating on the right side of the MPP.
- If $\frac{dP_{pv}}{dV_{pv}} = 0 \rightarrow \frac{dI_{pv}}{dV_{PV}} = -\frac{I_{pv}}{V_{pv}}$, then the system is operating at the MPP.

The following figures depict the operating regions and the flow chart of the algorithm.

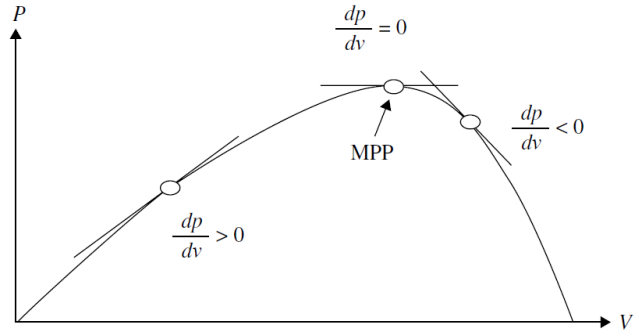

Figure 8: Incremental conductance operating region.

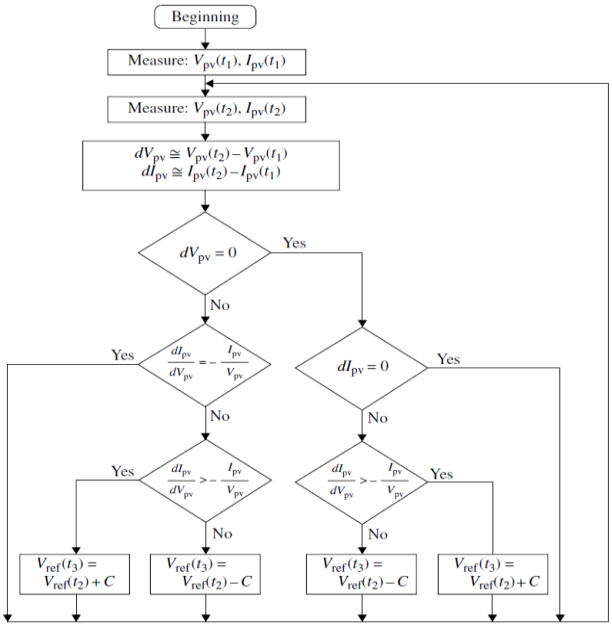

Figure 9: Incremental conductance algorithm for MPP.

C. ANN model

Intensely parallel, non-algorithmic information processing systems called artificial neural network (ANN) can learn the correlation between input and output variables. through examples, such as previously recorded data. It is composed of a set of neurons arranged into layers of input, hidden and output layers. Neurons accept inputs through their incoming connections, combines them, conducts a nonlinear operation, and then outputs the results through interconnected weighted links that pass the signal [24]. For this paper a feedforward multilayer neural network (FFNN) with backpropagation will be used. Information travels in a "feedforward" fashion from the input layer to the concealed layer and then to the output layer, meanwhile the backpropagation implies that the weights of the links are fine-tuned after each iteration which lesser the rate of error [24]. The transfer function operated by each neuron is given by a sigmoid function $f(Z_i)$.

$$f(Z_i) = \frac{1}{1+e^{Z_i}} \quad (15)$$

$$Z_i = \sum_{j=1}^{n} w_{ij} x_j + \beta_i \quad (16)$$

Where n is the number of input neuron, Z_i the sum of inputs weights, x_j is the input signal of the *jth* neuron of the input layer, w_{ij} is the weight defined between neuron j and i at the hidden layer while β_i is the error defined at neuron i. Figure 8 shows a diagram of FFNN.

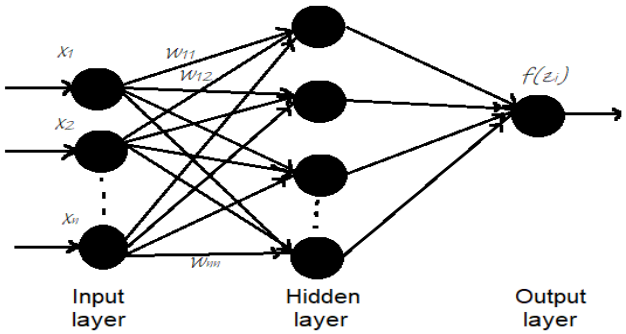

Figure 10: Feedforward neural network diagram.

IV. Evaluation Metric, Results, and Discussion

A. Evaluation metric

The simulation of our system is based on ground data collected from the Southern African Universities Radiometric Network (SAURAN). Data collected to train our ANN model are hourly irradiation and temperature from Pretoria for the year 2022, the data considered in the timespan are from 6:00 am to 7:00 pm while the algorithm used for ANN is Levenberg-Marquardt. A partial presentation of the weather conditions is given in the following tables.

Table1: Variations of irradiation and temperature.

UPR - GIZ University of Pretoria		
TmStamp	GHI_Avg	Temp_Avg
	W/m^2	Deg C
TmStamp	Avg	Avg
01/01/2022 06:00:00	12,80	15,00
01/01/2022 07:00:00	102,18	15,60
01/01/2022 08:00:00	395,17	16,92
01/01/2022 09:00:00	671,16	19,21
01/01/2022 10:00:00	860,21	20,95
01/01/2022 11:00:00	1027,49	22,41
01/01/2022 12:00:00	1004,00	23,52

Our model is predicting the output current from a single panel Kyocera KC200GT where the measured output current is formulated by the empirical mathematical model given in the following equation [33]:

$$I_{out}(t) = \frac{P_m\left(\frac{G(t)}{G_{STC}}\right) - \alpha_p(T(t) - T_{STC})}{V(t)_{PV}} \quad (17)$$

$$\alpha_p = \frac{Kv}{V_{mp}} \quad (18)$$

Where α_p is the temperature coefficient of power, the maximum power is P_m, V and T are the PV voltage and temperature, while T_{STC} is the temperature at standard test conditions (STC). Kv is the temperature coefficient of V_{OC} and V_{mp} is the maximum voltage at STC. The prediction' results are given by the following figure:

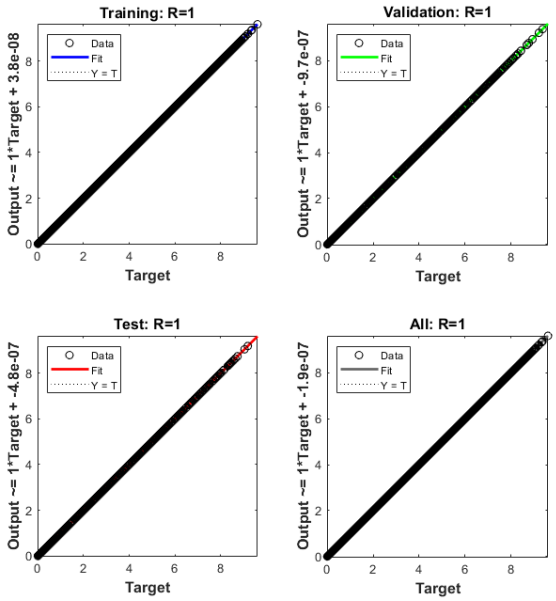

Figure 11: Statistical regression plots.

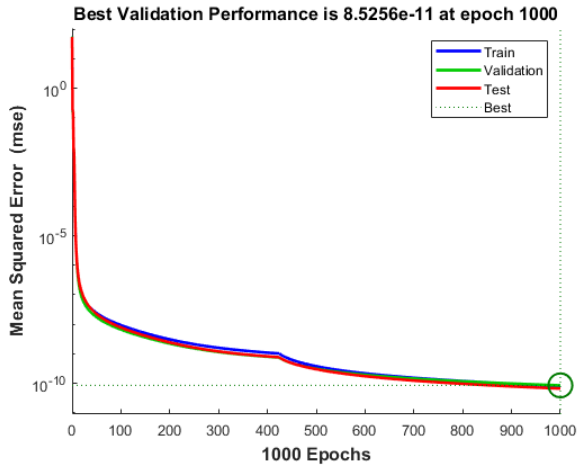

Figure 12: Best validation means square error (MSE).

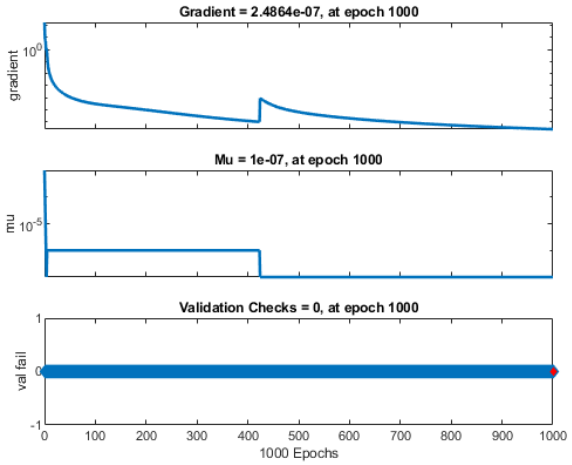

Figure 13: Training state validation.

Figure 11 describes a statistical regression plot which determines the accuracy of our model during training and validation process. A value of statistical analyses R closer or equals to 1 means that the performance of our model is very accurate, which is validated again with a means square error of $8{,}5256 * 10^{-11}$ on figure 12. Figure 13 depicts the validation test of ANN algorithm, the test was run under 1000 epochs and derived a gradient test value of $2{,}4864^{-7}$, which shows how close the optimal solution is to the true minimum. A lower gradient value indicates that the algorithm is converging successfully and taking tiny, steady steps towards the ideal solution. The algorithm successfully adjusts parameters to reduce the discrepancy between projected and real values, leading to enhanced accuracy. The validation check is at 0 and denoted an effective training and generalization of the data. These parameters denote the accuracy of our algorithm.

The boost converter is designed to double the input voltage at the output while trying to preserve the required input power at the output by conservation of energy. The following table describes the considerations of our boost converter.

Table 2: Boost converter considerations.

Boost converter parameters		
Description	**Value**	**Unit**
Inductance (L)	6,750 x10^-4	H
Input Capacitance (C1)	0,0270	F
Output Capacitance (C2)	0,0135	F
Load Resistance (RL)	100	Ω
Switching frequency	100	kHz
Efficiency (η)	94,07	%

B. Results and discussion

Our first hypothesis for MPP tracking includes algorithms such as P&O, IC, hybrid P&O with ANN and

hybrid IC with ANN conducted under uniform weather conditions for a temperature of 45 °C and irradiance of 1000 W/m^2. The results from table 3 depict that using P&O or IC algorithm, the maximum power is 182,8 W for a convergence time of 0,133 seconds. Meanwhile when each method is combined with ANN, the maximum power remains at 182,8 W and the convergence time to this peak is 0,158 seconds due to process complexity. However, this complexity is rewarded with an efficiency of 98% for each algorithm ANN combined with P&O or ANN combined with IC. Meanwhile the efficiency of P&O or IC algorithm is measured at 92%. The tracking efficiency is defined as the percentage of the sum of measured power over the sum of theoretical maximum power on a specific period, the equation is given by:

$$(\%)\eta_{mpp} = \frac{\Sigma_{t1}^{t2} P}{\Sigma_{t1}^{t2} Pmax} * 100 \quad (18)$$

The following table demonstrates the results of the simulation.

Table 3: Models characteristics under uniform conditions.

	Uniform conditions 1000 W/m2 @45°C			
Models	Power Max (W)	Convergence Time (s)	Frequency(kHz)	Efficiency (%)
P&O	182,8	0,133	5 kHz	92
IC	182,8	0,133	5 kHz	92
Hybrid (P&O,ANN)	182,8	0,158	5 kHz	98
Hybrid (IC,ANN)	182,8	0,158	5 kHz	98

A comparative analyses of our results was made in table 4 with findings of authors in [14], it follows that our algorithm converge faster to its maximum power point despite little loss in efficiency.

Table 4: Comparative analyses under uniform conditions.

	Uniform conditions 1000 W/m2 @45°C				
	Proposed model		Other authors [14]		
	P&O / IC	Hybrid(IC,ANN)	P&O	IC	Fuzzy Logic
Efficiency (%)	92	98	96,98	97	99,22
Time (s)	0,133	0,158	2,95	2,97	0,8

The following figures show the graph's behaviors of each algorithm. On figure 14 the fluctuations of maximum power using the conventional methods under constant irradiance are against the expected theoretical maximum power graph. We observe a quick convergence to MPP at $0{,}133\ s$ using conventional method against $0{,}158\ s$ for hybrid method, which takes a little longer on figure 15 where the hybrid behavior is depicted against theoretical maximum power. However, the hybrid method presents a more predictable behavior with a seemingly constant output power with an efficiency of 98% against 92% for conventional method.

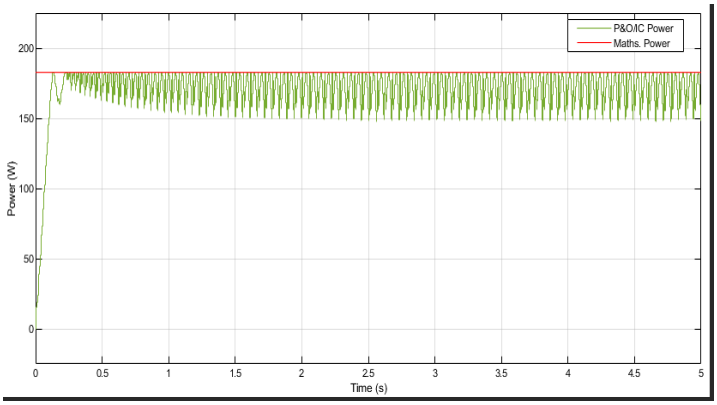

Figure 14: P&O/IC vs Theoretical maximum power under uniform conditions.

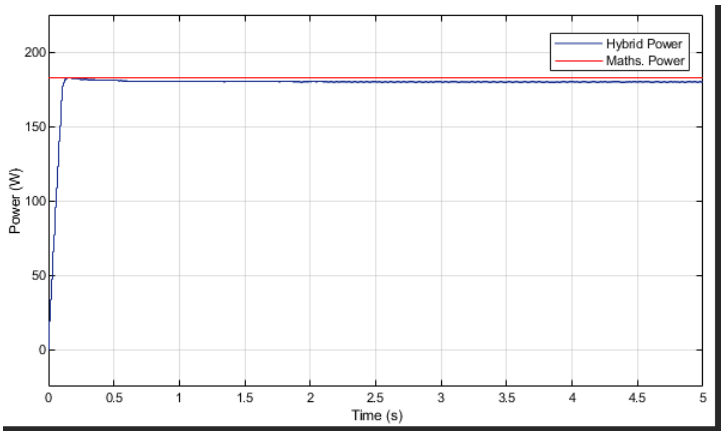

Figure 15: Hybrid method vs Theoretical maximum power under uniform conditions.

Our second hypothesis for MPP tracking includes the previous cited algorithms under variable weather conditions for a change of irradiances of 1000 W/m^2, 800 W/m^2, 600 W/m^2, 400 W/m^2, 200 W/m^2, over a temperature of 25 °C. the results from table 5 show that the efficiency of IC and P&O are 94% whereas the hybrid methods (ANN ft IC or ANN ft P&O) efficiency is 93%. The time of convergence to MPP during fast changing irradiance is $1{,}013\ \mu s$ for hybrid method on figure 17 and $4{,}274\ ms$ for IC/P&O method on figure 16. On figure 18, the conventional methods (IC/P&O) demonstrates some fluctuations around the true MPP given by the theoretical graph however these fluctuations were getting less present as the irradiance was decreasing which increased the power efficiency at 94% meanwhile on figure 19 the same comparison was made with the hybrid method which depicts a high accuracy at a high irradiance but gradually decrease as the irradiance reaches 200 W/m^2 with a total power efficiency of 93%.

The following table and figures depict our results.

Table 5: Models characteristics under variable conditions.

Variable conditions 1000 Wm2, 800 W/m2, 600 W/m2, 400 W/m2, 200 W/m2 @25°C		
Models	**Efficiency %**	**Tracking times (s)**
P&O	94	0,004274
Inc	94	0,004274
P&O Ann	93	0,000001013
Inc Ann	93	0,000001013

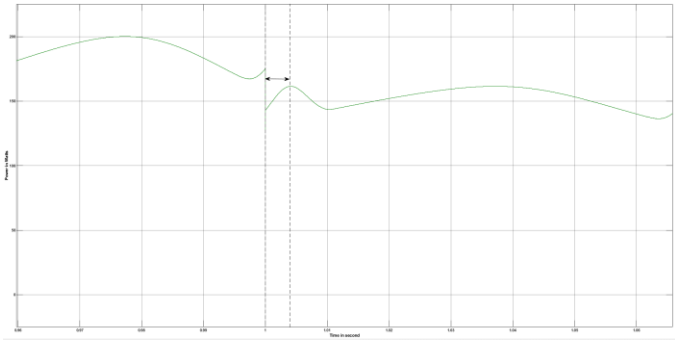

Figure 16: Convergence time for IC/P&O under variable conditions.

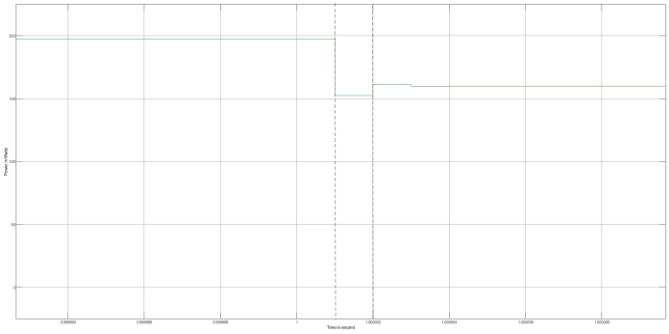

Figure 17: Convergence time for hybrid method under variable conditions.

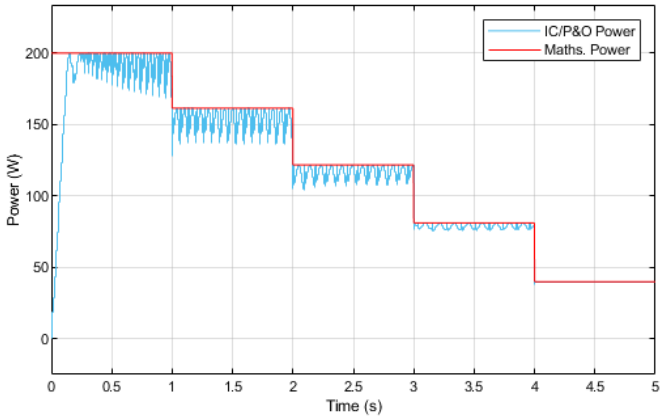

Figure 18: P&O/IC method vs Theoretical maximum power under variable conditions.

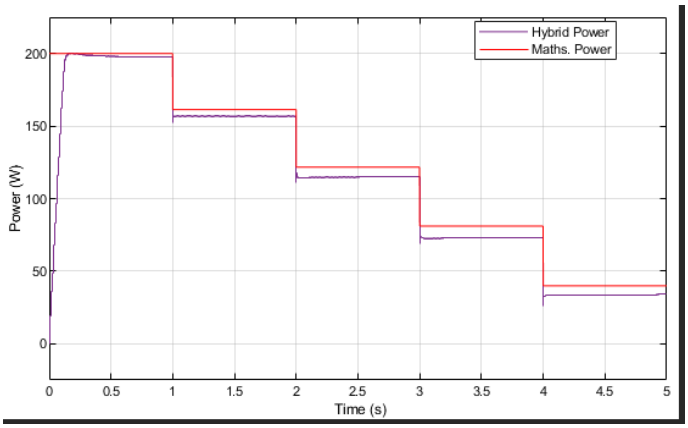

Figure 19: Hybrid method vs Theoretical maximum power under variable conditions.

V. Conclusion

This paper proposes a hybrid solution for tracking the maximum power under uniform and variable weather conditions. A neural network was designed to be combined with conventional methods (P&O or IC) to form the hybrid algorithm using Simulink MATLAB. A boost converter was also modelled to double the output voltage to preserve the input power of the PV panel from the law of energy conservation. Simulations for P&O and IC methods yields to the same results under uniform conditions with a response time of 0.133 sec and a tracking of 4.274 ms during fast changing conditions. In addition, they both yield an efficiency of 92% and 94% under uniform and variable weather conditions respectively. The hybrid solution made with P&O or IC provides a response time of 0,158 sec and an efficiency of 98% under uniform irradiances. However, this efficiency drops to 93% with a fast-tracking response of 1,013 μs for variable radiations.

The proposed solution was compared to other research and found to be better for tracking changes with a very good efficiency as the comparison in table 4 described. However, this solution can be improved with non-exhaustive optimization techniques such as particle swarm optimization (PSO) or genetic algorithm optimization. In addition, the structure of the system can be mounted on a boost-buck converter for better power efficiency and could also be associated with other renewable energy such as wind or thermal energy.

Declaration

The authors hereby declare that this work has no conflicts of interests according to our knowledge.

REFERENCES

[1] S. Allahabadi, H. Iman-Eini, and S. Farhangi, "Fast artificial neural network based method for estimation of the global maximum power point in photovoltaic systems," *IEEE Transactions on Industrial Electronics*, vol. 69, pp. 5879-5888, 2021.

[2] S. Qamar, M. Ahmad, B. Oryani, and Q. Zhang, "Solar energy technology adoption and diffusion by micro, small, and medium enterprises: sustainable energy for climate change mitigation," *Environmental Science and Pollution Research*, vol. 29, pp. 49385-49403, 2022.

[3] S. Jirakiattikul, T. T. Lan, and K. Techato, "Advancing households' sustainable energy through gender attitudes towards rooftop PV installations: A case of the Central Highlands, Vietnam," *Sustainability*, vol. 13, p. 942, 2021.

[4] S. Essakiappan, P. Enjeti, R. S. Balog, and S. Ahmed, "Analysis and mitigation of common mode voltages in photovoltaic power systems," in *2011 IEEE Energy Conversion Congress and Exposition*, 2011, pp. 28-35.

[5] P. Manganiello, M. Balato, and M. Vitelli, "A survey on mismatching and aging of PV modules: The closed loop," *IEEE Transactions on Industrial Electronics*, vol. 62, pp. 7276-7286, 2015.

[6] S. R. Pendem and S. Mikkili, "Modeling, simulation, and performance analysis of PV array configurations (Series, Series-Parallel, Bridge-Linked, and Honey-Comb) to harvest maximum power under various Partial Shading Conditions," *International journal of green energy*, vol. 15, pp. 795-812, 2018.

[7] R. F. Coelho, F. M. Concer, and D. C. Martins, "A MPPT approach based on temperature measurements applied in PV systems," in *2010 IEEE International Conference on Sustainable Energy Technologies (ICSET)*, 2010, pp. 1-6.

[8] A. Ali, K. Almutairi, S. Padmanaban, V. Tirth, S. Algarni, K. Irshad, *et al.*, "Investigation of MPPT techniques under uniform and non-uniform solar irradiation condition–a retrospection," *IEEE Access*, vol. 8, pp. 127368-127392, 2020.

[9] F. Hyder, K. Sudhakar, and R. Mamat, "Solar PV tree design: A review," *Renewable and Sustainable Energy Reviews*, vol. 82, pp. 1079-1096, 2018.

[10] A. R. Jordehi, "Maximum power point tracking in photovoltaic (PV) systems: A review of different approaches," *Renewable and Sustainable Energy Reviews*, vol. 65, pp. 1127-1138, 2016.

[11] D. Routray, P. K. Rout, and B. K. Sahu, "A brief review and comparative analysis of two classical MPPT techniques," in *2021 International Conference in Advances in Power, Signal, and Information Technology (APSIT)*, 2021, pp. 1-6.

[12] M. Sarvi and A. Azadian, "A comprehensive review and classified comparison of MPPT algorithms in PV systems," *Energy Systems*, vol. 13, pp. 281-320, 2022.

[13] M. A. Younis, T. Khatib, M. Najeeb, and A. M. Ariffin, "An improved maximum power point tracking controller for PV systems using artificial neural network," *Przegląd Elektrotechniczny*, vol. 88, pp. 116-121, 2012.

[14] B. Bendib, H. Belmili, and F. Krim, "A survey of the most used MPPT methods: Conventional and advanced algorithms applied for photovoltaic systems," *Renewable and Sustainable Energy Reviews*, vol. 45, pp. 637-648, 2015.

[15] M. A. Enany, M. A. Farahat, and A. Nasr, "Modeling and evaluation of main maximum power point tracking algorithms for photovoltaics systems," *Renewable and Sustainable Energy Reviews*, vol. 58, pp. 1578-1586, 2016.

[16] L. Xiaoping, Q. Yunyou, and S. SaeidNahaei, "A novel maximum power point tracking in partially shaded PV systems using a hybrid method," *International Journal of Hydrogen Energy*, vol. 46, pp. 37351-37366, 2021.

[17] S. Messalti, "A new neural networks MPPT controller for PV systems," in *IREC2015 the sixth international renewable energy congress*, 2015, pp. 1-6.

[18] Ö. Çelik, K. Zor, A. Tan, and A. Teke, "A novel gene expression programming-based MPPT technique for PV micro-inverter applications under fast-changing atmospheric conditions," *Solar Energy*, vol. 239, pp. 268-282, 2022.

[19] H. N. Zainudin and S. Mekhilef, "Comparison study of maximum power point tracker techniques for PV systems," 2010.

[20] K.-H. Chao, Y.-S. Lin, and U.-D. Lai, "Improved particle swarm optimization for maximum power point tracking in photovoltaic module arrays," *Applied energy*, vol. 158, pp. 609-618, 2015.

[21] S. Hesari, "Design and implementation of maximum solar power tracking system using photovoltaic panels," *International Journal Of Renewable Energy Research*, vol. 6, pp. 1221-1226, 2016.

[22] M. Danandeh, "Comparative and comprehensive review of maximum power point tracking methods for PV cells," *Renewable and Sustainable Energy Reviews*, vol. 82, pp. 2743-2767, 2018.

[23] J. P. Ram, N. Rajasekar, and M. Miyatake, "Design and overview of maximum power point tracking techniques in wind and solar photovoltaic systems: A review," *Renewable and Sustainable Energy Reviews*, vol. 73, pp. 1138-1159, 2017.

[24] T. Khatib and W. Elmenreich, *Modeling of photovoltaic systems using Matlab: Simplified green codes*: John Wiley & Sons, 2016.

[25] J. Wu, X. Chen, and L. Wang, "Design and dynamics of a novel solar tracker with parallel mechanism," *IEEE/ASME Transactions on Mechatronics*, vol. 21, pp. 88-97, 2015.

[26] A. Nadeem and A. Hussain, "A comprehensive review of global maximum power point tracking algorithms for photovoltaic systems," *Energy Systems*, vol. 14, pp. 293-334, 2023.

[27] J. Ramos Hernanz, J. Campayo Martin, I. Zamora Belver, J. Larranaga Lesaka, E. Zulueta Guerrero, and E. Puelles Perez, "Modelling of photovoltaic module," in *International conference on renewable energies and power quality (ICREPQ'10)*, 2010, pp. 23-25.

[28] L. Castaner and S. Silvestre, *Modelling photovoltaic systems using PSpice*: John Wiley and Sons, 2002.

[29] A. Hayat, D. Sibtain, A. F. Murtaza, S. Shahzad, M. S. Jajja, and H. Kilic, "Design and Analysis of Input Capacitor in DC–DC Boost Converter for Photovoltaic-Based Systems," *Sustainability*, vol. 15, p. 6321, 2023.

[30] M. H. Rashid, *Power electronics handbook*: Butterworth-heinemann, 2017.

[31] B. Hauke, "Basic calculation of a boost converter's power stage," *Texas Instruments, Application Report November*, pp. 1-9, 2009.

[32] J. Antonanzas, N. Osorio, R. Escobar, R. Urraca, F. J. Martinez-de-Pison, and F. Antonanzas-Torres, "Review of photovoltaic power forecasting," *Solar Energy*, vol. 136, pp. 78-111, 2016.

[33] E. O. Ekogha and P. A. Owolawi, "Supervised Learning-Based PV Output Current Modeling: A South Africa Case Study," Singapore, 2023, pp. 537-546.